

International Journal of Modern Physics C
© World Scientific Publishing Company

Lattice spin simulations of topological defects in biaxial nematic films with homeotropic surface alignment

GOURIPEDDI SAI PREETI*, CLAUDIO ZANNONI

*Dipartimento di Chimica Industriale "Toso Montanari",
Viale Risorgimento 4, 40136 Bologna, Italy*

CESARE CHICCOLI, PAOLO PASINI

INFN, Sezione di Bologna, Via Irnerio 46, 40126 Bologna, Italy

VANKA S.S. SASTRY

School of Physics, University of Hyderabad, Hyderabad. India.

We present a detailed Monte Carlo study of the effects of biaxiality on the textures of nematic films with specific homeotropic boundary conditions. We have used the Straley generalized Hamiltonian for a wide range of biaxial parameters and the differences obtained in the polarized microscopy images are analysed for the various cases.

Keywords: Computer simulation, Monte Carlo, Biaxial Nematics, Topological Defects.

PACS: 61.30.Cz, 61.30.Gd, 61.30.Jf, 62.20.dq

1. Introduction

Biaxial nematic (BN) liquid crystals have attracted considerable attention¹ since the early 1970s, when Freiser first predicted the existence of these phases^{2,3}, partly because the numerous unsuccessful attempts¹ at synthesizing them posed doubt on their very existence. The interest in these materials has recently been renewed and has widely spread after experimental evidence of phase biaxiality in low molar mass nematic liquid crystals was put forward not only for lyotropics⁴ and polymers^{5,6}, but also for various low molar mass thermotropic systems. In particular bent core oxadiazole based mesogens^{7,8} and tetrapodes have been extensively investigated using various techniques like NMR⁷ and infrared spectroscopy^{9,10}. From the theoretical point of view a considerable amount of effort has been deployed by Virga and coworkers^{11,12,13,14} to successfully put the mean field level description of these phases on a rigorous basis, starting from a rather general, even if purely orientational pair potential due to Straley¹⁵, finding stability ranges for various parameterizations^{11,12,13,14}. Extensive simulation studies have also been performed

*presently: Kothari post-doctoral fellow, CMSD, University of Hyderabad, Hyderabad, India.

on the same type of second rank biaxial potential with lattice models, i.e. assuming particle positions to be confined to lattice sites, to investigate the biaxial phase and its transitions both for the special case of dispersive interactions^{16,17,18,19,20} or for more general parameterizations²¹ going beyond the inevitable approximations of effective field treatments. Computer simulations at coarse grain, molecular level, resolution with off lattice models, have also demonstrated the possibility of forming BNs even in competition with the formation of smectic or crystal biaxial phases²². Off lattice simulations are expected to be significative for unraveling the structural features of biaxial mesogens at the molecular level and for helping in the design and optimization of devices towards the technological deployment of biaxial materials²³. The experiments done for detecting phase biaxiality have been based on various spectroscopic and optical techniques. Optical probing of topological defects is of special interest, since the symmetry difference of biaxial and uniaxial order might lead to significant differences in the properties of defects in BN and uniaxial nematics²⁴ and thus in the observed polarized microscopy images, that for nematics correspond to the so called Schlieren textures²⁴. Chandrasekhar et al.^{25,26} noticed that polarizing microscope textures of their candidate BNs contained only defects of half integer and never of integer strength. Since the uniaxial nematic phase shows defects of both types, the observation was suggested as a diagnostic test for biaxiality²⁵ and this suggestion was also recently reconsidered by Picken et al.²⁷. Similar observations were also made by us performing a simulation of defects for a model Hamiltonian based on a special case of the general Straley hamiltonian: that corresponding to London dispersion forces¹⁷. In that case it was seen that initially four brush defects appeared which then evolved and disappeared by splitting into defects with only two brushes²⁸. More recently we have done a simulation of a BN film in a planar geometry²⁹ with random anchoring conditions by using a more general hamiltonian^{15,11} which considers various parameterizations of the potential and accordingly gives a richer phase diagram²¹. In this case the defects visible when the biaxial liquid crystal film was confined between two surfaces imposing planar degenerate anchoring were either of four or two brushes depending on the biaxial parameters and not just two brushes as observed using the dispersion model²⁸. It should be noticed that, topologically, integer defect lines are not forbidden in BNs³⁰, thus the appearance of defects should depend not only on the symmetry of the nematic phase, but also on the relative values of elastic constants, on the film thickness and mainly on surface anchoring. There is therefore a strong need for a detailed analysis of the influence of different boundary conditions on the appearance of the type of defects. For this reason, also stimulated by a recent experimental work³¹ on bent-core molecular systems where the substrates implement homeotropic, rather than planar, alignment, we have performed a detailed simulation study of a BN film with homeotropic surface anchoring using the generalized Straley lattice Hamiltonian for a complete set of biaxial parameters. The aim of the present study is to investigate the appearance and the type of topological defects that can be produced.

2. The model systems

The model we employ is based on the most general purely orientational pair potential between two rigid particles with biaxial D_{2h} symmetry, that was originally put forward by Straley¹⁵ and recently revisited, see e.g.^{11,12,13}. For a cubic lattice with nearest neighbor interactions, as assumed here, and in the notation introduced by Romano^{19,20}, as well as by Virga and coworkers¹³, the hamiltonian has the following form:

$$U_{ij} = \varepsilon\{-G_{33} + \Gamma(G_{11} - G_{22}) - \Lambda[2(G_{11} + G_{22}) - G_{33}]\} \quad (1)$$

where $G_{mn} \equiv P_2(\mathbf{u}_m^i \cdot \mathbf{u}_n^j)$ and \mathbf{u}_m^i , with $m = 1, 2, 3$, are the orthogonal unit vectors representing the axis system of particle i . ε denotes a positive constant setting the temperature and the energy scales, $T^* = k_B T / \varepsilon$, P_2 is a Legendre polynomial. The potential in Eq. 1, that depends on the two parameters Γ , Λ can be considered as the second rank, $L=2$, contribution in a even more general expansion over Wigner rotation matrices of rank L . To relate Γ and Λ to the length L , breadth B and width W of brick-like molecules is a difficult task (see Ref.²¹); when Γ and Λ vanish the model reduces to the well known Lebwohl-Lasher potential³² which correctly reproduces the uniaxial nematic isotropic phase transition^{32,33}.

As mentioned above we have studied a film where the alignment at the bottom and top surface in the biaxial film is homeotropic. To implement that we have considered two additional layers at the top and at the bottom of the system where the molecules have their long axes aligned homeotropically along z and are kept frozen during the simulation. The strength of the anchoring at the surface is modelled in the hamiltonian introducing a coupling parameter J scaling the interaction between one molecule belonging to the liquid crystal and the second one belonging to the substrate. The boundary conditions at the four lateral faces of the simulation box are left free. The updating of the lattice is performed according to the classic Metropolis Monte Carlo procedure³⁴. The simulation of the optical polarizing microscope textures were produced by means of a Müller matrix approach^{35,36}, assuming the molecular domains represented by the spins to act as retarders on the light propagating forward through the sample³⁷. The following arbitrary but reasonable parameters were employed for computing the optical textures: film thickness $d = 5.3 \mu\text{m}$, refractive indices $n_x = 1.51$, $n_y = 1.54$ and $n_z = 1.61$, and light wavelength $\lambda_0 = 545 \text{ nm}$. The light retarded by the liquid crystal molecules is observed through crossed polarizers placed at $\pi/4$ and $3/4\pi$ with respect to x . A pixel by pixel intensity map is obtained and the calculation is then repeated over a number (typically 500) of different configurations sampled around a certain evolution step to give the average intensity maps shown with a grey coding in the figures (between black: no light, and white: light through)^{37,38}.

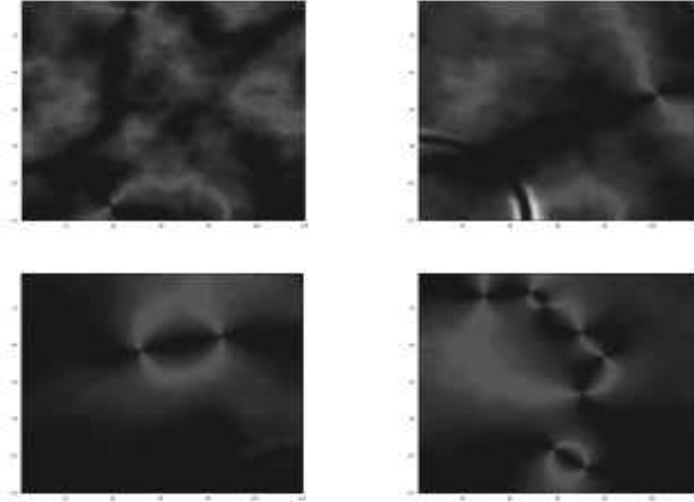


Fig. 1. Polarized microscopy textures as obtained by Monte Carlo simulation of a homeotropic film with biaxial parameters $\Gamma = 0.6$ and $\Lambda = 0.5$ respectively for different values of anchoring strength J . The images are taken after 100k evolution cycles for $J = 1.0$ (top left), $J = 0.5$ (top right), $J = 0.2$ (bottom left) and $J = 0.1$ (bottom right).

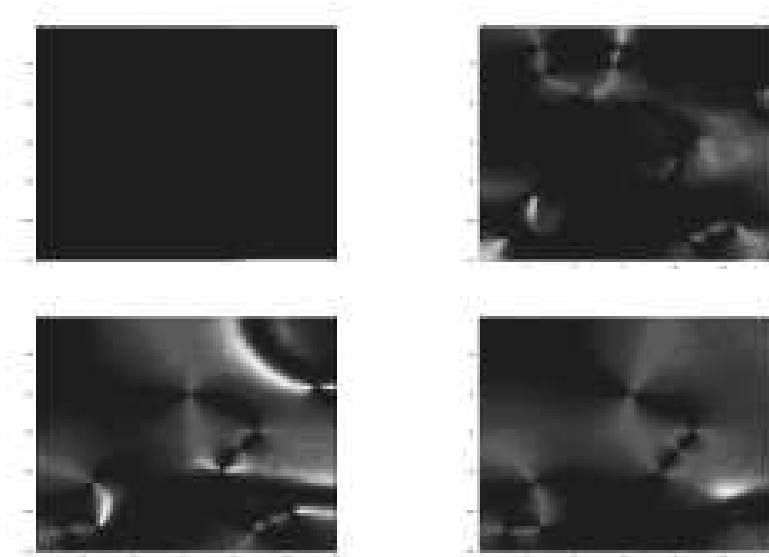


Fig. 2. Polarized microscopy textures as obtained by Monte Carlo simulation of a homeotropic surface system with biaxial parameters $\Gamma = 0.3$ and $\Lambda = 0.6$ taken after 10k (top left), 20k (top right), 50k (bottom left), 100k (bottom right) evolution cycles for an anchoring strength $J = 0.1$.

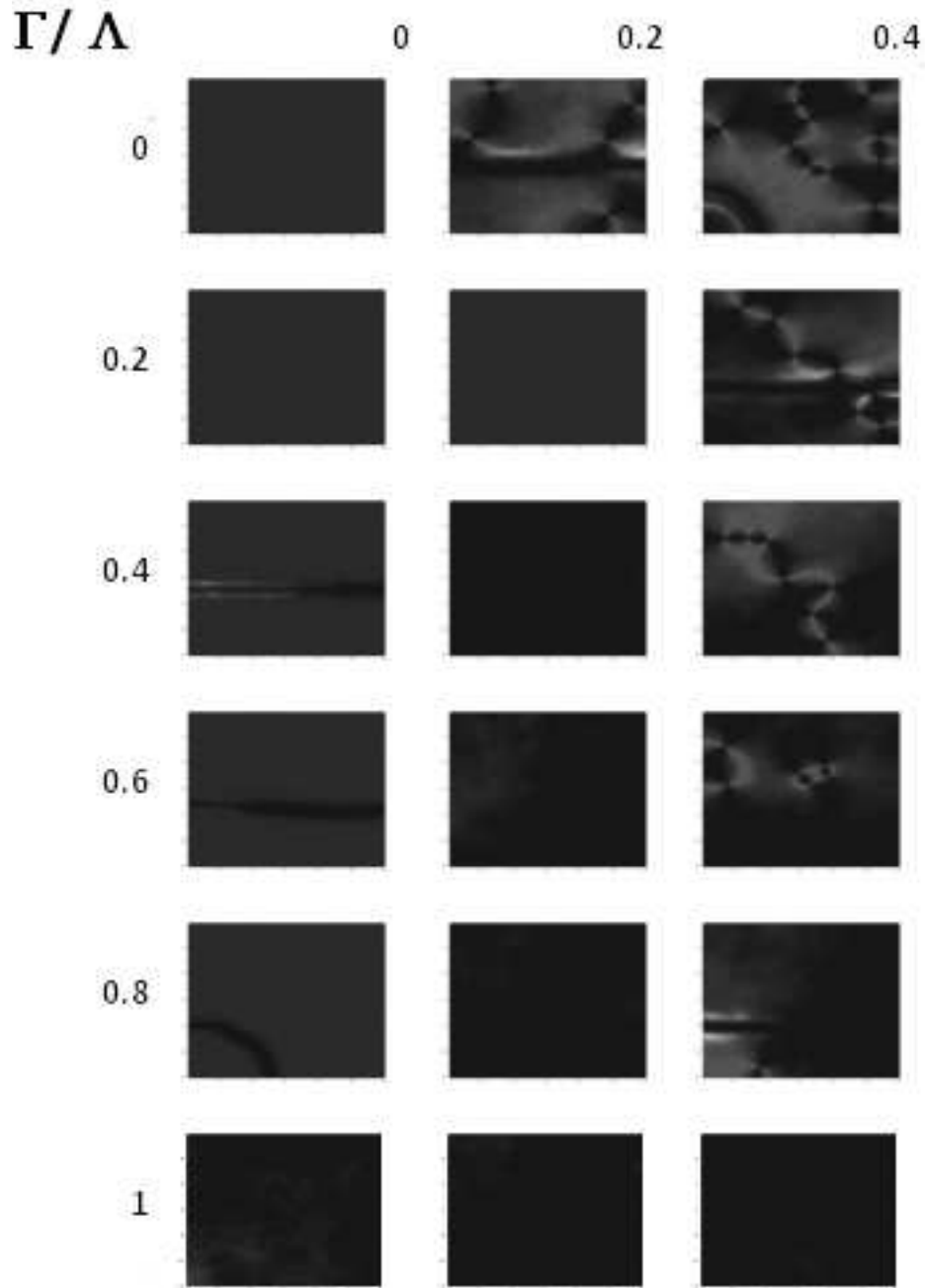


Fig. 3. A selection summary of the textures as obtained from MC simulations for the homeotropic surfaces case after the same number of cycles (100k) for the different values of the parameter Γ and $\Lambda = 0., 0.2, 0.4$.

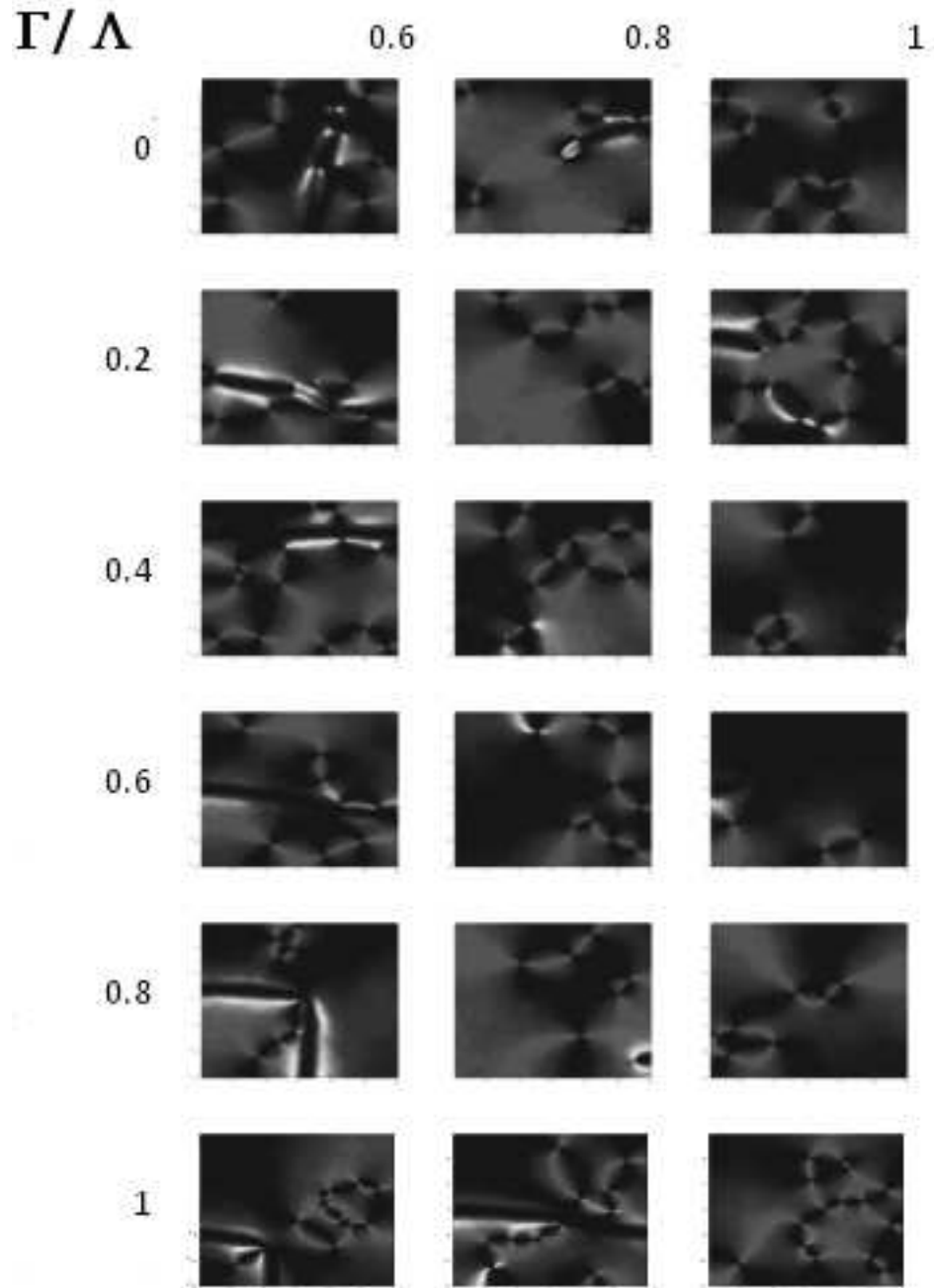


Fig. 4. As Fig. 3 for the different values of the parameter Γ and $\Lambda = 0.6, 0.8, 1$.

3. Simulations and results

Since in real experiments the network of defects appears when the thickness of the film is sufficiently large we have at first investigated this aspect. To do this we have considered a $120 \times 120 \times 10$ system and instead of increasing the film thickness we have chosen to decrease the strength of the anchoring with the surfaces because we have shown in previous works that reducing the substrate anchoring strength is equivalent to increase the film thickness in the simulation^{28,38}. This approach has obvious practical advantages from the simulations point of view, since it avoids resorting to an increase of the number of particles in the system, and the unavoidable enhancement in the demands of computer time, with the consequent advantage of making it feasible to increase the number of runs which can be performed. To simulate the cooling from an isotropic phase to a biaxial one, as done in the real experiment³¹, we have then chosen to start from an initial configuration of the system with completely random orientation of the molecular long axes. We have chosen the biaxial parameters $\Gamma = 0.6$ and $\Lambda = 0.5$, the temperature to $T^* = 0.1$ (temperature at which every set of biaxial parameters gives a biaxial phase) and the anchoring strength J of the substrates was then decreased systematically in steps of 0.1 from 1.0 to 0.1. All the simulated textures develop from the initial "black" state and we have observed stable defects appearing for the lower values of the anchoring strength, as shown in Fig. 1. Each defect is characterized by two brushes emerging from its core. The texture evolves as the system anneals, but the defects do not disappear even in the longest runs performed (200000 Monte Carlo sweeps or cycles, where a cycle is a full lattice update) even though they occasionally migrate outside the sample. An example of the evolution of the simulated textures is reported in Fig. 2 for the biaxial parameters $\Gamma = 0.3$ and $\Lambda = 0.6$, and anchoring strength $J = 0.1$.

It is apparent for the two choices of biaxial parameters presented in Figs 1 and 2 only two brushes defects with topological charge $\pm 1/2$ appear. To test if only this type of defects are produced for this particular geometry with homeotropic anchoring at the surfaces we have then performed a detailed study varying Γ and Λ each in the range $[0,1]$ with a interval $\Delta = 0.1$ for a total of one hundred cases. For all this simulation scan we have used an anchoring strength $J = 0.1$.

A representative selection of the images obtained for the different values of Γ and Λ is reported in Fig. 3 and Fig. 4. It seems that the number of defects increases as Γ and Λ increase. We can also see that, for low values of Λ , defects are not produced over all the Γ domain. In particular for very low values of Γ (0.0, 0.1) defects did not appear on equilibration. On increasing the Λ value chains of two brush defects were observed.

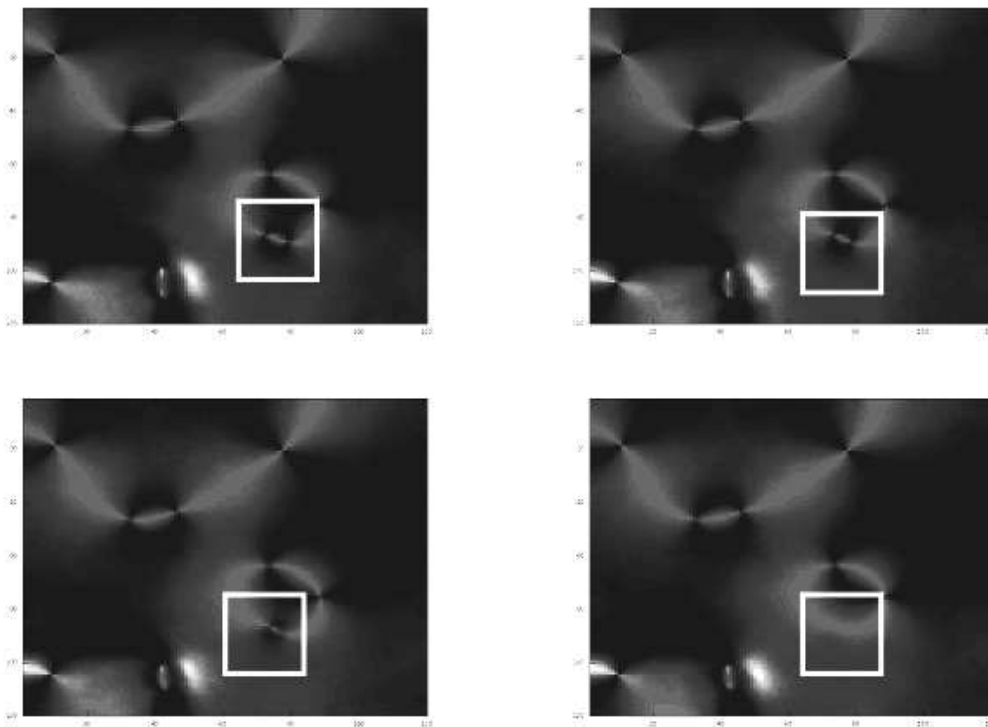


Fig. 5. Example of annihilation (within the square) of two brushes defects with opposite charge as obtained from MC simulation of a biaxial film with parameters $\Gamma = 0.6$ and $\Lambda = 0.7$. The images are taken at 95 (top right), 96 (top left), 97 (bottom right) and 98 (bottom left) cycles.

Increasing the value of Γ it appears clearly that the absence of defects persists also for larger values of the second parameter up to $\Lambda = 0.4 - 0.5$ for $\Gamma = 1$ (Figs. 3 and 4, last row) and for the higher values of Λ , very long chains of defects with charges $\pm 1/2$ appear on equilibration. It is obvious from these studies that defects of integral charges were not visible over the complete range of Λ and Γ . Differently from the planar long axis geometry, where the substrates produce a random planar alignment for the long axes, the two brushes defects are not produced by a splitting of a four brushes point defect but are directly created by the system. The defects are created during the evolution and they can eventually annihilate each other if they are of opposite charge as can be seen in Fig.5.

The director structure plots, (Fig. 6), shown as snapshots of the spins of a single layer, confirm the presence of the two brush defects in these systems. An interesting feature observed here was the presence of an equal number of positively and negatively charged defects. Again, also comparing with the experimental results^{25,26,30}, these defects can disappear by collapsing into another of opposite charge over a long period of time.

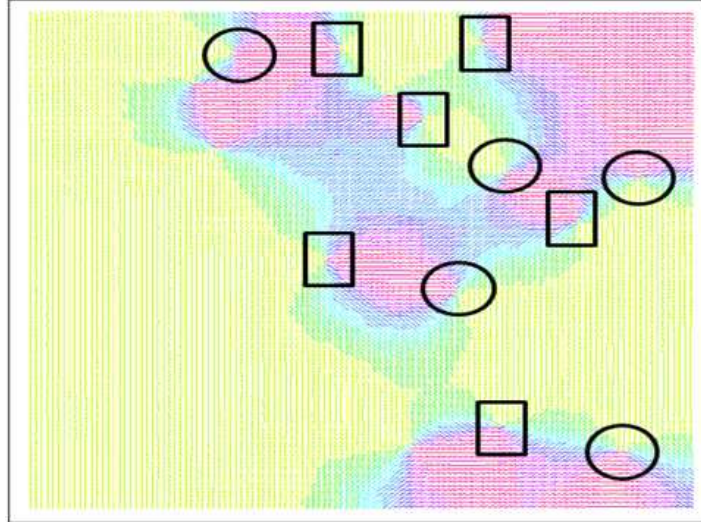


Fig. 6. Distribution of the secondary director in the eighth layer of the homeotropic system with $\Gamma = 0.6$, $\Lambda = 0.8$ where pairs of half integer defects were initially observed (the circle represent defects with $-1/2$ and square $+1/2$ charges respectively.)

4. Conclusions

We have performed an extensive Monte Carlo study of a BN film with homeotropic boundary conditions by using a full Straley pair potential which takes into account the biaxiality of the molecules. We have simulated a $120 \times 120 \times 10$ biaxial liquid crystal film system with homeotropic boundaries and considered different combinations of biaxial parameters to verify their relative importance on the formation of various optical patterns and in particular looking for the onset of a short axis Schlieren texture. We have shown that defects of only half integral topological charge occur in a BN confined between homeotropic substrates, in agreement with the experimental study of Chandrasekhar^{25,26,31}. Even if the presence of two brushes defects cannot be considered as a unique test of biaxiality^{27,39,40} we have shown that this type of disclinations of strength $|s| = 1/2$ is the only one that practically appears in the case of homeotropic alignment and that the stability of these defects depends on the value of Γ and Λ .

Acknowledgements

This work was supported by the EU-STREP Project "Biaxial Nematic Devices" (BIND) FP7-216025 C.Z. is grateful to MIUR PRIN "Novel ordered systems for high response molecular devices" (2011-2013), while C.C. and P.P. thank INFN (grant I.S. BO62) for support.

References

1. G.R. Luckhurst, *Nature* **430**, 413 (2004)
2. M.J. Freiser, *Phys. Rev. Lett.* **24**, 1041 (1970)
3. M.J. Freiser, *Mol. Cryst. Liq. Cryst.* **14**, 165 (1971)
4. L.J. Yu and A. Saupe, *Phys. Rev. Lett.* **45**, 1000 (1980)
5. F. Hessel and H. Finkelmann *Polymer Bull.* **15**, 349-352 (1986)
6. K. Severing, E. Stibal-Fischer, A. Hasenhindl, H. Finkelmann and K. Saalwachter, *J. Phys. Chem. B* **110**, 15680-15688 (2006)
7. L. A. Madsen, T. J. Dingemans, M. Nakata and E. T. Samulski, *Phys. Rev. Lett.* **92**, 145505 (2004)
8. B.R. Acharya, A. Primak and S. Kumar, *Phys. Rev. Lett.* **92**, 145506 (2004)
9. K. Merkel, A. Kocot, J.K. Vij et al., *Phys. Rev. Lett.* **93**, 237801 (2004)
10. J.L. Figueirinhas, C. Cruz, D. Filip et al., *Phys. Rev. Lett.* **94**, 107802 (2005)
11. A.M. Sonnet, E.G. Virga and G.E. Durand, *Phys. Rev. E* **67**, 061701 (2003)
12. G. De Matteis, S. Romano and E.G. Virga, *Phys. Rev. E* **72**, 041706 (2005)
13. F. Bisi, E.G. Virga, E.C. Gartland et al., *Phys. Rev. E* **73**, 05170 (2006)
14. F. Bisi, G.R. Luckhurst and E.G. Virga, *Phys. Rev. E* **78**, 02171 (2008)
15. J.P. Straley, *Phys. Rev. A* **10**, 1881 (1974)
16. G.R. Luckhurst and S. Romano, *Mol. Phys.* **40**, 129 (1980)
17. F. Biscarini, C. Chiccoli, P. Pasini et al., *Phys. Rev. Lett.* **75**, 1803 (1995)
18. C. Chiccoli, P. Pasini, F. Semeria et al., *Int. J. Mod. Phys. C* **10**, 469 (1999)
19. S. Romano, *Physica A* **337**, 505 (2004)
20. L. Longa, P. Grzybowski, S. Romano et al., *Phys. Rev. E* **71**, 05171 (2005)
21. G. Sai Preeti, K.P.N. Murthy, V.S.S. Sastry, C. Chiccoli, P. Pasini, R. Berardi, and C. Zannoni, *Soft Matter* **7**, 11483 (2011)
22. R. Berardi and C. Zannoni, *J. Chem. Phys.* **113**, 5971 (2000)
23. R. Berardi, L. Muccioli and C. Zannoni, *J. Chem. Phys.* **128**, 024905.1 (2008)
24. P. G. de Gennes and J. Prost, *The Physics of Liquid Crystals*, 2nd ed. (Clarendon Press, Oxford, 1993)
25. S. Chandrasekhar, G.G. Nair, D. Rao, S.K. Prasad, K. Praefcke and D. Blunk, *Current Science* **75**, 1042 (1998)
26. S. Chandrasekhar, G.G. Nair, D. Rao et al., *Liq. Cryst.* **24**, 67 (1998)
27. S.J. Picken, T.J. Dingemans, L.A. Madsen, O. Francescangeli and E.T. Samulski, *Liq. Cryst.* **39**, 19 (2012)
28. C. Chiccoli, I. Feruli, O.D. Lavrentovich, P. Pasini, S.V. Shiyonovskii and C. Zannoni, *Phys. Rev. E* **66**, 030701.1 (2002)
29. G. Sai Preeti, C. Chiccoli, P. Pasini, V.S.S. Sastry and C. Zannoni, *Mol. Cryst. Liq. Cryst.*, in press (2013)
30. M. Kleman, *Points, Lines and Walls, In Liquid Crystals, Magnetic Systems, and Various Ordered Media*, (Wiley, New York, 1982)
31. M. Nagaraj, Y.P. Panarin, U. Manna, J.K. Vij, C. Keith and C. Tschierske, *Appl. Phys. Lett.* **96**, 011106 (2010)
32. P.A. Lewohl and G. Lasher, *Phys. Rev. A* **6**, 426(1972).
33. U. Fabbri and C. Zannoni, *Molec. Phys.* **58**, 763, (1986).
34. N. Metropolis, A.W. Rosenbluth, M.N. Rosenbluth, A.H. Teller and E. Teller, *J. Chem. Phys.* **221**, 1087 (1953)
35. A. Killian, *Liq. Cryst.* **14**, 1189 (1993)
36. R. Ondris-Crawford, E.P. Boyko, B.G. Wagner, J. H. Erdmann, S. Zumer and J.W. Doane, *J. Appl. Phys* **69**, 6380 (1991)
37. E. Berggren, C. Zannoni, C. Chiccoli, P. Pasini, and F. Semeria, *Phys. Rev. E* **50**,

- 2929 (1994)
38. O.D. Lavrentovich, P. Pasini, C. Zannoni and S. Zumer (eds.), *Defects in Liquid Crystals: Computer simulations, Theory and Experiments* (Kluwer, Dordrecht, 2001).
 39. K. Van Le, M. Mathews, M. Chambers, J. Harden, Q. Li, H. Takezoe, and A. Jkli, *Phys. Rev. E* **79**, 030701(R) (2009)
 40. B. Senyuk, Y.-K. Kim, L. Tortora, S.-T. Shin, S.V. Shiyanovskii, and O.D. Lavrentovich, *Mol. Cryst. Liq. Cryst.* **540**, 20 (2011).